Measuring Turbulence Characteristics of Artificial Biofilms using LDV and High Speed Photography

S.K. Ng[1] and J.M. Walker[2]

[1]School of Engineering
University of Tasmania, Hobart, Tasmania 7000, Australia

[2]National Centre for Maritime Engineering & Hydrodynamics
Australian Maritime College, University of Tasmania, Launceston, Tasmania 7250, Australia

Abstract

The structure of the flow over filamentous biofilms was investigated using an 80 mm long idealised biofilm streamer inserted in a recirculating water tunnel. Previous studies have found that the presence of streamers affects the turbulence structure of the boundary layer including changing the turbulence intensity, Reynolds stress profiles, skin friction coefficient and boundary layer thickness.

To fully quantify these changes high speed photography was coupled with boundary layer profiles obtained using laser Doppler velocimetry at several freestream velocities. The images were processed using photogrammetric techniques to track the motion of a filament and quantify the movement of the tip in relation to the boundary layer. This data was then correlated with the turbulence results from the boundary layer traverses. Results for turbulence behind a single streamer are compared to results for a smooth reference surface.

The maximum displacement of the streamer tip increased with increasing freestream velocity, and three distinct stroke patterns of the streamer tail were observed. Significant disturbances to both the mean velocity profile and the turbulence intensity were measured in the region of streamer movement (1.3–9 mm from the wall) and the presence of the streamer resulted in a large increase in wake strength.

Introduction

The presence of biofilms at solid-liquid interfaces causes large drag penalties due to the increase in surface friction, which is of concern to a wide range of industries including hydropower generation, water reticulation and shipping. Filamentous biofilms have been observed to cause higher friction losses than their low-form gelatinous biofilm counterparts [1, 7, 9, 12]. Previous studies on filamentous biofilms include those by Picologlou et al. [9], Lewkowicz & Das [7], Stoodley et al. [14], Schultz [12], Andrewartha (et al.) [1-3] and Taherzadeh [15].

Stoodley et al. [14] found that the oscillation amplitude of filamentous biofilms increased sigmoidally with flow velocity. The oscillatory frequency of a streamer was well correlated to the Strouhal number, suggesting that the streamer vibration may be triggered by vortices shedding in vicinity of streamers. Taherzadeh et al. [15] conducted a two-dimensional computational simulation of transient coupling between the flow mechanics and a single streamer at various streamer lengths. The formation of a Kármán vortex street downstream of the streamer tail was identified as the key trigger of streamer periodic oscillations. Simulation indicated a sigmoidal amplitude-frequency relationship that confirms Stoodley et al.'s [14] experimental results.

Boundary layer measurements over surfaces with artificial filamentous streamers [2, 3, 7] and real filamentous biofilms [12] found increases in local skin friction coefficient, c_f; thickening of the boundary layer and increases in the shape factor; increases in the wake strength; elevated turbulence intensity (normalised by the freestream velocity, U) over either part of or the whole boundary layer depending on the streamer density; elevated Reynolds normal stresses; and an outwards shift in the peak of the Reynolds shear stress profile that corresponded to the maximum extent of streamer movement.

The present study extends the previous work by examining the boundary layer structure immediately behind a single streamer in conjunction with high speed photography to capture the motion of the streamer.

Experimental Facilities and Method

Test Surface

A single 80 mm long artificial streamer was glued to a smooth painted test plate (see Figure 1). The wool filament was glued so that its free end was leaning downstream, even without flow, as observed with real biofilm filaments (similarly to Lewkowicz & Das [7]). The tail of the streamer was tagged with black permanent marker to allow easy tracking. Wool was used because its fibre has a relatively high flexibility, elastic recovery, and bendability [5].
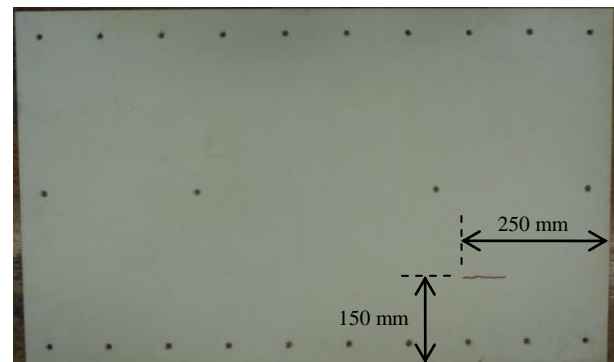

Figure 1 Wool streamer glued to the smooth-coated test plate.

Boundary Layer Profiles

Boundary layer velocity profiles were obtained directly behind the streamer using the University of Tasmania Water Tunnel [10]. The recirculating water tunnel has a 2.2 m × 0.6 m × 0.2 m working section, with 997 mm × 597 mm test plates suspended from the lid to form the roof. The freestream turbulence intensity is approximately 1% and U was varied from 1.0–2.0 m/s. One-dimensional turbulent boundary layer velocity profiles were obtained using a laser Doppler velocimetry (LDV) system where the streamwise velocity component, u, was measured using a pair

of red beams (660 nm). The flow was seeded with 10 μm hollow glass spheres and 10,000 random samples were obtained at each of 70 positions in the boundary layer.

Bradshaw's method, as described by Winter [17], was used to analyse the boundary layer data. A reference point ($y^+ = 100$ for which $u^+ = 16.2$) on the inner-law curve (equation 1) was taken, where $y^+ = yu^*/\nu$, y is the distance from the wall, $u^+ = u/u^*$ and u^* is the wall shear velocity. By taking a range of values of u^+ a curve of u/U versus yU/ν can be drawn. The value of u/U at the intersection of this curve with the measured velocity profile gives c_f (equation 2). A minor wall origin correction, ε, was applied by fitting the data to Spalding's equation (3) in the region $y^+ < 100$ [13]. The wake strength, Π, was found by fitting equation (4) to the data, as suggested by White [16].

$$u^+ = \kappa^{-1}\ln\left(y^+\right) + C \tag{1}$$

$$c_f = 2\left(\frac{u^*}{U}\right)^2 = 2\left(\frac{u}{U}\right)^2 \bigg/ \left(\frac{u}{u^*}\right)^2_{ref} \tag{2}$$

$$y^+ = u^+ + e^{-\kappa C}\left(e^{\kappa u^+} - 1 - \kappa u^+ - \frac{\left(\kappa u^+\right)^2}{2!} - \frac{\left(\kappa u^+\right)^3}{3!} - \frac{\left(\kappa u^+\right)^4}{4!}\right) \tag{3}$$

$$\frac{U-u}{u^*} = -\frac{1}{\kappa}\ln\left(\frac{y+\varepsilon}{\delta}\right) + \frac{2\Pi}{\kappa}\cos^2\left(\frac{\pi}{2}\frac{y+\varepsilon}{\delta}\right) \tag{4}$$

where ν is the kinematic viscosity, κ is the von Kármán constant, taken to be 0.41 and C is the smooth wall log law constant, taken to be 5.0.

The data was corrected for velocity bias using transit time averaging. The effects of fringe bias and velocity gradient bias were investigated [1]; however, no corrections were found necessary. Repeatability tests were used to generate uncertainty estimates for all variables. Ten replicate boundary layer profiles were taken in order to determine the 95% confidence interval [4]. The resulting uncertainties in U, δ, θ and δ^*, u^* and c_f, ε, $\sqrt{\overline{u'^2}}/U$, $\overline{u'^2}/u^{*2}$ were ±0.2%; ±2.0%; ±1.5%; ±0.3%; ±3.0%; ±1.8%; and ±4%, respectively.

High Speed Photography

The rapid movement of the streamer was captured and recorded using a Kodak Motion Corder Analyzer SR-Series. The camera was mounted on a custom designed camera support to provide an adjustable camera position in three dimensions [8]. The videographic parameters are given in Table 1. Two halogen lamps were located underneath the tunnel working section to enhance the illumination level.

Parameter	Value
Shutter speed	1/500 s
Frame rate	125 frames per second
Aperture	5.6
Display size	521×240 pixels^2 (173.7×80 mm^2)
Focal length	0.47 m

Table 1: Photographic settings of the experiment

A 200×200 mm^2 calibration grid of mesh size 5×5 mm^2 was deployed in the water tunnel at zero flow at the same optical distance as the streamer and a photograph of it was taken [8]. Based on the image of the calibration grid as an input, a MATLAB program was developed to process the data and convert the time-trace streamer tail position from digital dimension (pixel) to physical length (mm) and rectify image distortion using an iterative piecewise texture mapping method and corner detection algorithm.

Motion tracking was conducted to extract the time and displacement coordinates of the marked streamer tail from the videos using a MATLAB based motion tracking program developed by Hedrick [6]. Full details of the image analysis process are given in Ng [8]. Ten replicate videos of the streamer motion were captured for each of the four freestream velocities (1.00 m/s, 1.25 m/s, 1.75 m/s and 2.00 m/s).

Results and Discussion

Streamer Movement from High Speed Photography

The tail of the streamer was tracked as described above and profiles of streamer motion in x and y coordinates are given in Figure 2 for the four freestream velocities, where the point (0,0) (not shown) represents the streamer attachment point and y = 0 mm represents the test plate. The profiles indicate that the streamer wall normal motion is much more significant than the streamer movement in the streamwise direction. Three distinct motion paths or strokes can be observed. The motion profile becomes more scattered as the flow velocity increases.

The frequency of the streamer tail position (in the wall normal direction) lying in each 1 mm band in the region 0–10 mm was examined in the form of a histogram for each freestream velocity (Figure 3). The distributions changed significantly from 1.00 m/s, where the streamer position had a bimodal distribution, to 2.00 m/s, where the streamer position was normally distributed. The histograms reveal a concentration of the streamer tail position in the region 6–7 mm from the wall at the lower freestream velocities.
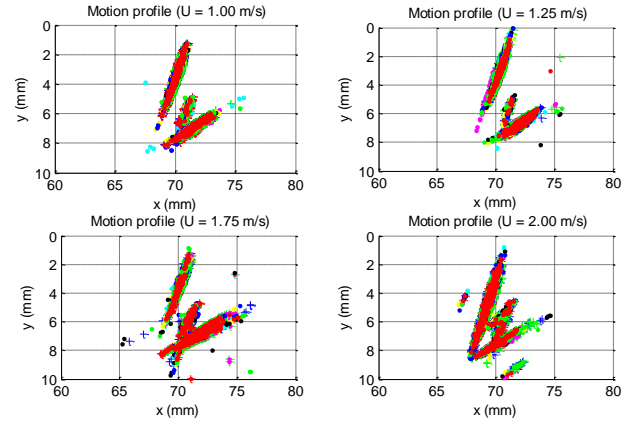

Figure 2 Ten replicate profiles of streamer tail position at different U (y = vertical location, x = horizontal location, 80 mm long streamer attached at (0,0)). Flow direction was from left to right.
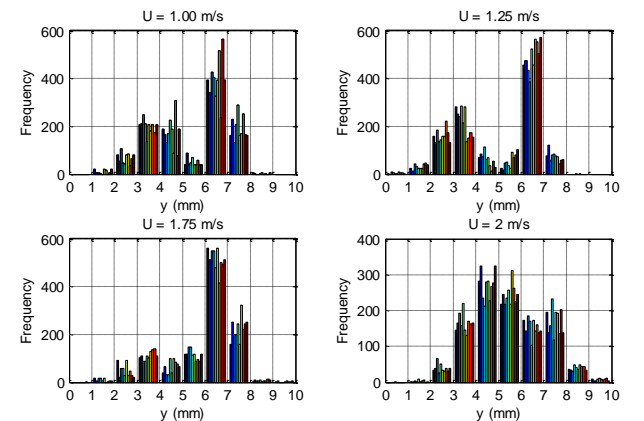

Figure 3 Vertical streamer tail position frequency histograms for ten replicate profiles of streamer motion at different U.

| Plate	U [m/s]	Re_θ	δ [mm]	δ^* [mm]	θ [mm]	H	Π	ε [mm]	u^* [m/s]	c_f
Streamer	1.00	3.31E3	32.3	4.75	3.46	1.37	0.74	0.15	0.038	0.00288
Streamer	1.25	4.14E3	32.1	4.77	3.53	1.35	0.72	0.13	0.047	0.00281
Streamer	1.75	5.56E3	33.5	4.51	3.41	1.32	0.57	0.09	0.065	0.00281
Streamer	2.00	6.49E3	32.6	4.53	3.39	1.34	0.72	0.08	0.072	0.00258
Smooth	1.00	2.93E3	31.6	4.38	3.31	1.32	0.29	0.02	0.042	0.00354
Smooth	1.25	3.48E3	31.3	4.19	3.18	1.32	0.29	0.02	0.052	0.00342
Smooth	1.75	5.02E3	35.2	4.17	3.25	1.28	0.22	0.04	0.070	0.00320
Smooth	2.00	5.55E3	32.2	4.06	3.16	1.29	0.29	0.04	0.079	0.00313

Table 2 Boundary Layer Parameters
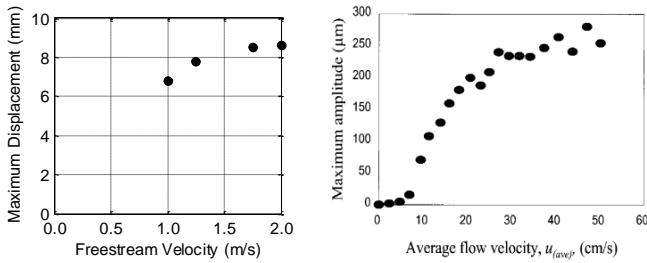
Figure 4 (a) Maximum vertical streamer displacement with U, (b) Maximum amplitude (half maximum displacement) of biofilm streamer from Stoodley [14] exhibiting a sigmoidal shaped curve

The maximum vertical streamer displacement exhibits a Reynolds number dependence as it increases with flow velocity as shown in Figure 4(a). The magnitude of the displacement appears to plateau as the freestream velocity approaches 2.00 m/s. This result supports the work of Stoodley et al. [14] who undertook measurements at much lower velocities and found that the maximum amplitude (defined as half the maximum displacement) increased with average flow velocity (see Figure 4(b).This may be the result of increased vortex shedding occurring at higher flow velocity (Reynolds number), at which the momentum force dominates the viscous force [14]. The streamer's material flexibility might restrict the amplitude [14].

Boundary Layer Parameters

Boundary layer parameters for each surface are given in Table 2 at four different freestream velocities. The streamer plate had a significantly stronger wake region (see Table 2 and Figure 5) and slightly elevated displacement and momentum thicknesses, which were also observed by Andrewartha & Sargison [2], Andrewartha et al. [3] and Lewkowicz & Das [7] for flows over pliable roughnesses.

Mean Velocity Structure

Mean velocity boundary layer profiles at four different freestream velocities are given in Figure 5 in log law form and in Figure 6 in velocity defect form. The streamer profiles sit well on the smooth wall log law curve, which indicates that the single streamer has not had a roughening effect on the boundary layer. The increase in wake strength over the smooth wall profile is evident in Figure 5. The velocity defect profiles (Figure 6) diverge from the smooth wall profile over the region 1.3–9.0 mm from the test plate which indicates that the presence of the streamer does locally change the mean velocity structure of the boundary layer in the region corresponding to streamer movement.
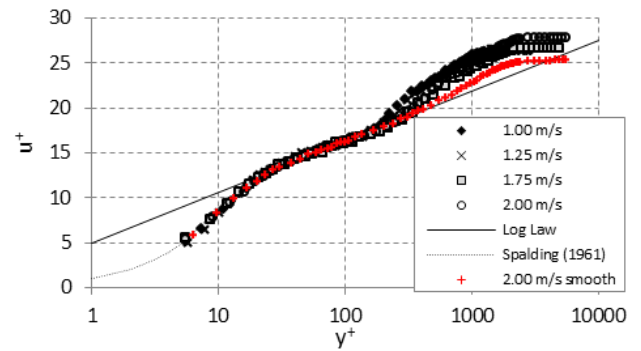

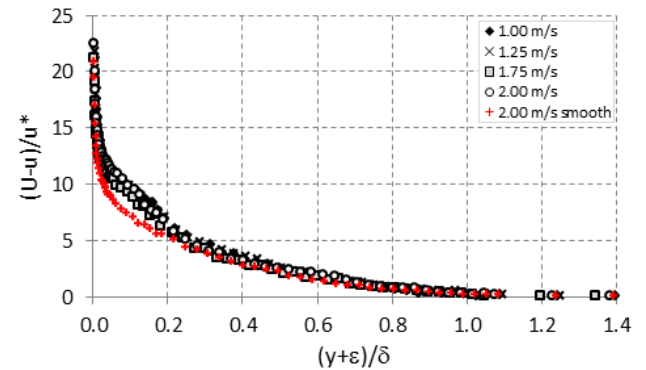Figure 5 Boundary Layer Mean Velocity Profiles in Inner Coordinates

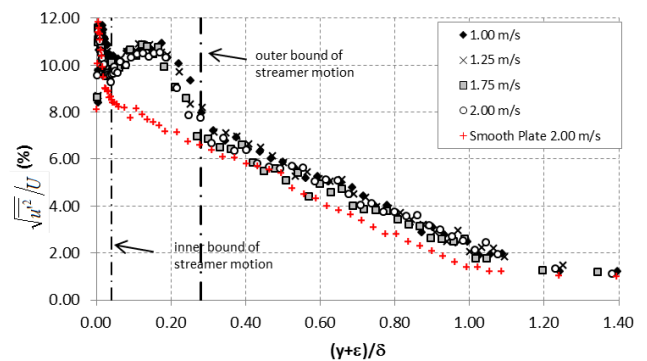
Figure 6 Velocity Defect Profiles

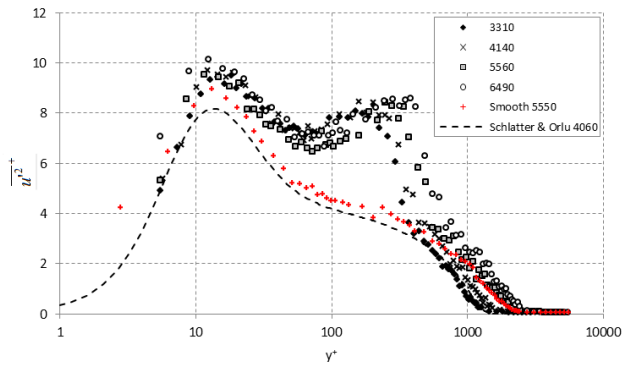Figure 7 Turbulence Intensity Profiles (normalised by the freestream velocity, U)

Figure 8 Streamwise Reynolds Normal Stress Profiles (normalised by the wall shear velocity, $u*$) at various Re_θ.

Turbulence Structure

Turbulence intensity profiles normalised by the freestream velocity are given in Figure 7. The data are compared to a smooth wall profile from the water tunnel. The turbulence intensity data for the streamer plate collapse well and are clearly elevated above the smooth wall data in the region $0.04 < (y+\varepsilon)/\delta < 0.28$ (1.3 mm $<$ y+ε $<$ 9 mm). The turbulence intensity in the very near wall region was not affected by the presence of the streamer. The turbulence intensity returned to approximately smooth wall values for $(y+\varepsilon)/\delta > 0.28$.

Streamwise Reynolds normal stress profiles are presented in Figure 8, along with smooth wall Direct Numerical Simulation data of Schlatter and Orlu [11]. The experimental smooth wall data follows the same trend as the DNS data. The streamer data is clearly elevated due to the presence of the streamer.

Previous results on an array of streamers [1, 3] noted a localised increase in streamwise turbulence intensity in the region $0.08 < (y+\varepsilon)/\delta < 0.4$. Results for a denser, staggered array of streamers [2] showed a much larger increase in streamwise turbulence intensity over a much greater proportion of the boundary layer. Lewkowicz & Das [7] also measured increases in turbulence intensity for flow over a pliable roughness over the entire boundary layer.

Conclusions

The coupling of high speed photography with one-dimensional turbulent boundary layer measurements has shown that the presence of a filament disrupts the structure of the boundary layer in the region immediately behind the streamer. Both the mean velocity and the turbulence structure were significantly altered in the region corresponding to the range of motion of the streamer. The presence of the streamer significantly increased the wake strength.

The streamer was observed to move in three distinct stroke patterns and the maximum displacement increased with increasing freestream velocity.

Acknowledgments

References

[1] Andrewartha, J., *The effect of freshwater biofilms on turbulent boundary layers and the implications for hydroelectric canals,* PhD Thesis, University of Tasmania, 2010.

[2] Andrewartha, J. and Sargison, J. *Turbulence and mean-velocity structure of flow over filamentous biofilms*, in IAHR 34th World Congress, 2011, Brisbane, Australia: Engineers Australia.

[3] Andrewartha, J., Sargison, J., Henderson, A., Perkins, K., and Walker, G. *The Effect of Freshwater Biofilms on Skin Friction Drag*, in 16th International Association of Hydraulic Engineering International Symposium on Hydraulic Structures, 2008, Nanjing, China.

[4] Coleman, H. and Steele, W., Engineering application of experimental uncertainty analysis, *AIAA Journal*, **33**(10), 1995, 1888-1895.

[5] Hatch, K.L., *Textile Science*. New York,1993.

[6] Hedrick, T., Software techniques for two- and three-dimensional kinematic measurements of biological and biomimetic systems, *Bioinspiration and Biomimetics*, **3**, 2008.

[7] Lewkowicz, A. and Das, D., Turbulent Boundary Layers on Rough Surfaces With and Without a Pliable Overlayer: A Simulation of Marine Fouling, *International Shipbuilding Progress, Marine Technology Monthly*, **32**, 1985, 174-186.

[8] Ng, S.K., *The Flow Physics of Filamentous Algae,* Honours Thesis, University of Tasmania, 2011.

[9] Picologlou, B.F., Zelver, N., and Charaklis, W.G., Biofilm growth and hydraulic performance, *ASCE J. Hydr. Div*, **HY5**, 1980, 733-747.

[10] Sargison, J., Barton, A., Walker, G., and Brandner, P., Design and calibration of a water tunnel for skin friction research, *Australian. J. Mech. Eng.*, **7**(2), 2009, 1-14.

[11] Schlatter, P. and Orlu, R., Assessment of direct numerical simulation data of turbulent boundary layers, *J. Fluid Mech*, **659**, 2010, 116 - 126.

[12] Schultz, M.P., Turbulent Boundary Layers on Surfaces Covered with Filamentous Algae, *J. Fluids Eng*, **122**, 2000, 357-363.

[13] Spalding, D.B., A Single Formula for the "Law of the Wall", *J. Appl. Mech.*, **28**, 1961, 455-458.

[14] Stoodley, P., Lewandowski, Z., Boyle, J.D., and Lapin-Scott, H.M., Oscillation characteristics of biofilm streamers in turbulent flowing water as related to drag and pressure drop, *Biotechnology and Bioengineering*, **57**(5), 1998, 536-544.

[15] Taherzadeh, D., Picioreanu, C., Kuttler, U., Simone, A., Wall, W., and Horn, H., Computational Study of the Drag and Oscillatory Movement of Biofilm Streamers in Fast Flows, *Biotechnology and Bioengineering*, **105**(3), 2010, 600-610.

[16] White, F.M., *Viscous Fluid Flow*, 2nd ed., McGraw-Hill,1991.

[17] Winter, K.G., An outline of the techniques available for the measurement of skin friction in turbulent boundary layers, *Prog. Aero. Sci.*, **18**, 1977, 1-57.